Proceedings of the

WINTER COLLEGE ON FUNDAMENTAL NUCLEAR PHYSICS

Volume 3

International Centre for Theoretical Physics, Trieste, Italy
7 Feb-30 Mar 1984

Editors

K Dietrich
M Di Toro
H J Mang

World Scientific

THE INTRANUCLEAR CASCADE FOR HEAVY ION RELATIVISTIC COLLISIONS

J. Cugnon and J. Vandermeulen
Physics Department B5, Univeristy of Liège,
Sart Tilman, B-4000 Liège 1 (Belgium)

ABSTRACT

We introduce the intranuclear cascade model and discuss the background for its application to nucleus-nucleus collisions in the energy range of 1 GeV per nucleon.

The ingredients of the model as implemented in a numerical code are described. The following properties of the system in collision are discussed : matter density, energy distribution of the particles, chemical composition. The results for the final proton spectra and for the yield and spectra of produced pions and kaons are given and compared to experiment. The emission of deuterons is analysed in connection with entropy.

The place of the model in the framework of kinetic theory is discussed, and a comparison is made with hydrodynamics. Possible modifications and extensions of the model, with regard to the properties of the compressed nuclear matter, and to application at lower and higher energies, are presented.

1. INTRODUCTION

Heavy ion collisions at energies beyond a few 100 MeV per nucleon offer the prospect to study, especially in the more central events, the properties of nuclear matter at high excitation energy and probably at densities larger than the normal one. However the system which is formed during the collision has a very short lifetime and only the products can be observed after they have flown out of the collision zone. A theoretical step is therefore necessary to relate the measured quantities (mass spectra of fragments, momentum spectra and correlations, ...) to the reaction mechanism and to the properties of the system in collision.

The collision between two nuclei in the relativistic regime faces us with a very complicated problem. The nirvana of the theorist would be, in the words of Nix [1], a quantal relativistic time-dependent, many-body theory including all hadronic degrees of freedom. Clearly this ambition has to be scaled down to something tractable, via adequate simplifications and approximations.

The first hint in that direction is provided by the fact that at sufficiently high energy each nucleon of the projectile has a sufficiently small de Broglie wavelength to be able to resolve the nucleons of the target individually. One may therefore contemplate a kind of classical regime in which the nuclear collision is treated as a sequence of point-like events : nucleon-nucleon collisions.

This approach has been applied previously to investigate the interaction of high energy hadrons with nuclei [2]. The hadron projectile impinging on the nucleus is assumed to make successive independent collisions in the target, the struck nucleons colliding then with other nucleons, with the result that a cascade of nucleons moving through the nucleus builds up : this is the essence of the intranuclear cascade (INC) model.

Before coming to the intranuclear cascade for nucleus-nucleus collision, let us look more closely at the conditions of applicability of this kind of model. The following conditions have been pointed out by Ginocchio [3] :

a) the energy transferred into internal energy of the target must be large compared to the binding energy of the target to allow the formulation of the many-body scattering problem approximately in terms of hadron-nucleon scattering amplitudes ;

b) if the radius R of the target nucleus is large with respect to the mean free path λ of the projectile, then many scatterings take place inside the nucleus and the interference terms between different scattered waves tend to cancel out ; this condition is more easily reached in a nucleus-nucleus collision than in a hadron-nucleus collision ;

c) if the mean free path of the incident particle λ is much larger than the de Broglie wavelength λ_B then the scattered wave will approximately reach its asymptotic value before the next scattering and a classical treatment of the scattering becomes reasonable ;

d) a last condition has to be fulfilled in order for the schematic picture of zero duration collisions separated by straight line trajectories to hold ; it can be formulated in two slightly different forms :

d.1) if the mean free path λ is larger than the interparticle distance d, the scattering from different nucleons in the nucleus can be assumed to be approximately independent from each other ;

d.2) the time intervals between successive scatterings must be much larger than the interaction times. Equivalently, the interaction radius r_s , at least the one associated with large momentum transfers, must be smaller than the average interparticle distance.

Both statements (d) amount to a condition of low density, in the sense that, if each nucleon is pictured as a small sphere of radius equal to the interaction range the total nuclear volume must be large compared to the sum of the proper volumes.

The above conditions may be summarized in the following inequalities :

$$E/A \gg B \quad , \tag{1.1}$$

$$\lambda_B, r_s < d < \lambda < R \quad , \tag{1.2}$$

where B is the binding energy per nucleon. Figure 1, which compares different characteristic lengths and characteristic energies of the system, shows that conditions (1.1)-(1.2) for the validity of the INC picture (or, in other words, of a quasi-classical multiple scattering model) are realized in the energy range around 1 GeV per nucleon. However, the numerical values are such that the inequalities involving d and λ are marginally satisfied. Therefore, one should expect non negligeable corrections to the INC model, at least for some observables (we indicate below some of these corrections). One reason to persevere is given by the remarkable success of the INC model, by far the most successful model in the GeV/A range, and by the fact that the alternative classical approach, namely hydrodynamics, is even in worse shape, as we explain in Section 4.

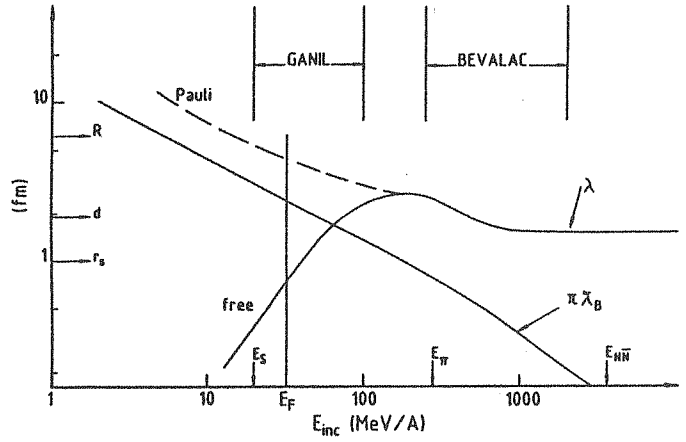

Figure 1.

Scale of different parameters for a system of two colliding nuclei. The lengths are defined in the text. The mean free path λ is computed from the free proton-proton cross section. The dashed line is an estimate of the correction due to the Pauli principle (see ref. 4). The quantity E_S is the kinetic energy associated to the sound velocity, E_F is the Fermi energy, E_π and $E_{N\bar{N}}$ are thresholds for production.

The extension of the INC approach to the collision of two nuclei is in principle straightforward. The larger number of pairs of particles with large relative momenta is a favourable situation for the classical approximation since phase space will be populated more extensively and therefore the cancellation of phase relations will be more effective.

Under the heading of INC models for heavy ion collisions stand calculations (or numerical codes) which are significantly different on the technical ground. Two main categories of treatments exist. The first one handles the target nucleus as a continuous medium as in the nucleon- or hadron- nucleus case whereas the projectile nucleus is a collection of nucleons ; the nucleons of the target are singled out as individual entities only once a collision has taken place. This asymmetrical situation presents a difficulty of principle. In a nucleon-nucleus collision it is reasonable to assume that the projectile and the cascading nucleons move through a medium of constant density since they propagate at a speed which is certainly larger than the one of a density perturbation. But a rapid investigation shows that it is certainly no longer the case for the collision of two nuclei of comparable sizes. Some "rearrangement" of the density may be assumed to take place as the nuclear collision proceeds but this seems a rather artificial procedure. The most representative codes of this group are the old VEGAS code, now known as the Yariv-Fraenkel code [5]) and the Toneev code [6]).

The second category of INC models treats projectile and target in a completely symmetric way, both being a collection of nucleons. This approach, by treating all nucleons with an equal status, incorporates quite naturally the interactions between the cascading particles and yields automatically the evolution of the density, a quantity of much theoretical interest. From now on, we shall refer to this latter type of treatment.

In the studied energy range one has to include in the

interaction between two nuclei not only elastic scattering but also particle production, essentially pion production. This type of interaction plays an essential role in the transformation of translational (kinetic) energy into excitation energy (heat) in the collision zone. The treatment of pion production as well as the other features of the implementation of the cascade will now be described in detail in Section 2. For specific details we shall constantly refer to the Liège code [7,8]) ; for a comparison between the main ingredients of different codes, see ref. [9]).

In Section 3, we will present the most significant results obtained within the INC model and discuss their implications on the physics of the reaction process. In Section 4, we will investigate the theoretical basis of the INC model and its connection with the hydrodynamical approach. We will also say a few words on its possible improvements. Finally, Section 5 will contain the conclusion.

2. DESCRIPTION OF THE INC MODEL

This section describes the main structure of the code developed in Liège and its ingredients. The following procedure is applied to each event (run) :

a) The impact parameter is fixed and the system is set up in the form of two touching spheres (radius : $1.12\ A^{1/3}$ fm) containing nucleons with positions and momenta given randomly, according to a uniform distribution and the Fermi gas law, respectively ; the Fermi momentum is 270 MeV/c. Each nucleus is defined in its own rest frame at this stage.

b) The nuclei are given their initial momenta by Lorentz boosting [Let us assume we work in the c.m. of the collision]. The shapes of the nuclei are accordingly Lorentz contracted into ellipsoïds.

c) The nuclear process is constructed by a succession of binary scatterings among the particles in the system. The trajectory of each nucleon (in general each hadron) is a straight line in absence of interaction. To find out which pair is bound to interact next, at what place and at what instant all pairs of trajectories are inspected and their time of closest approach (if any) is determined. For the pair which is the first to reach its closest distance of approach d_{min}, a test is made to find out if the interaction takes place. If the condition $d_{min} \leq (\frac{\sigma}{\pi})^{\frac{1}{2}}$ (where σ is the total cross-section for the interacting pair at its c.m. energy) is fulfilled, the scattering is assumed to take place instantaneously ; new momenta (and new identity in the case of inelastic scattering) are attached to the colliding particles. The scanning of the times of closest distances of approach is then resumed to find out the time and place of the next scattering, and so on ...

d) Technically, scattering is treated in the c.m. of the colliding pair. Whether it is elastic or inelastic is fixed by a random choice, according to the ratio of the cross sections. For nucleon-nucleon elastic scattering, the two angles ϑ (polar, with respect to the direction of the momentum) and φ (azimuthal) are chosen randomly according to, for ϑ :

$$\frac{d\sigma}{dt} \propto \exp\,(A(s)\cdot t) \qquad (2.1a)$$

$$t = -\,2q^2(1 - \cos\vartheta) \qquad (2.1b)$$

where A(s) is a function adopted to fit the slope derived from experiment,
and for φ, to a uniform distribution in the interval $[0,2\pi]$.
A(s) corresponds to almost isotropic scattering (Coulomb neglected) below T = 300 MeV (lab. energy for an incident nucleon on a nucleon at rest). The forward peak develops rapidly when energy increases : A(s) is about equal to $3(\mathrm{GeV/c})^{-2}$ at 0.6 GeV and to $5(\mathrm{GeV/c})^{-2}$ at 1 GeV ; it then

increases less rapidly at higher energy. The mean value of the scattering angle is given approximately by $\cos\vartheta = 0.41$ at 0.6 GeV and 0.79 at 1 GeV.

Energy and momentum are conserved at each collision, but angular momentum is not. Soft collisions ($\sqrt{s} < 1.925$ GeV) are neglected.

e) Up to incident energies of about 2 GeV/nucleon the predominant non-elastic process is the production of one pion. This is incorporated in the model through the inclusion of the Δ (1.232 GeV/c^2) isobar. The production of a pion is assumed to take place through the two-step process :

$$N + N \rightarrow N + \Delta \qquad (2.2)$$

$$\Delta \rightarrow N + \pi \quad . \qquad (2.3)$$

This is supported by the fact that the experimental properties of the NN system display a dominance of the resonant channel near the threshold of pion production. The Δ is treated as a particle with hadronic properties and before decaying after a finite ($\tau = \frac{\hbar}{\Gamma} = 1.6$ fm/c) lifetime it is apt to scatter. The following reactions are therefore included :

$$NN \rightarrow NN \quad , \quad N\Delta \rightarrow N\Delta \quad , \quad \Delta\Delta \rightarrow \Delta\Delta \quad , \quad NN \rightleftarrows N\Delta \quad , \quad \Delta \rightleftarrows N\pi \,. \qquad (2.4)$$

The last reactions in reverse order provide the mean to handle pion absorption in a nucleus without resorting to three or more-particle reactions since the absorption of a pion by a single free nucleon is forbidden by energy and momentum conservation.

For inelastic scattering Δ-production, a definite mass for the Δ is chosen according to the Breit-Wigner shape (with cut wings) ; the choice may have to be repeated if the mass does not allow to ensure the kinematical conditions. The final momenta are obtained in a way similar to above.

The effective threshold is just below T_{lab} = 300 MeV

($\sqrt{s}$ = 2.02 GeV) ; the inelastic cross section rises rapidly and becomes equal to the elastic one near T_{lab} = 0.9 GeV ($\sqrt{s}$ = 2.28 GeV) ; beyond, the inelastic cross section is slowly increasing and the elastic one slowly decreasing ; they make up an almost constant total cross section of 45 mb.

f) Once a Δ is formed, its effective lifetime is chosen randomly according to the exponential law $e^{-t/\tau\gamma}$, where τ is its proper time. The Δ is allowed to scatter during its lifetime. After this duration it is forced to decay (isotropically in its proper frame) into a pion and a nucleon.

g) The pion is assumed to propagate freely until it comes close enough (same criterion $d \leq (\frac{\sigma}{\pi})^{\frac{1}{2}}$ as above) to a nucleon, in which case they give birth to a Δ-isobar, whose mass is determined uniquely by kinematics. The formation cross section has a Breit-Wigner shape in accordance with the experimental πN cross section.

Points c) to g) above describe (see original references for more details) how the collision process is unfolded, how the sequence of binary processes (including Δ decay and formation) develops. This process is followed until the rate of reactions becomes negligible because the system has diluted too much. The remaining Δ's at that time are then forced to decay.

Due to the explosive nature of nucleus-nucleus collisions, in the GeV/A range, the potential well effects are neglected. The described model may thus be seen as a limiting gas dynamics picture. We will indicate below the observables which may be influenced by the potential well effects. The latter are included in the code developed by Kitazoe et al. [10]), which however neglects some inelastic effects.

The Pauli principle is neglected in the Liège code, which is more or less justified by the rapid dispersion of the nucleons in the available phase space. The soft collisions which are disregarded in this code take partly the Pauli principle into account, as explained in ref. [11]).

The whole procedure (a)-(g) is repeated several times and physical quantities are obtained by ensemble averaging. The number of runs is determined by the required accuracy. We will now characterize in a few words the output of the INC calculations, forgetting production processes for the sake of simplicity. The output can then be represented as a collection of 6 A quantities (A being the total baryon number) :

$$\{\vec{r}_1,\ldots,\vec{r}_A,\vec{p}_1,\ldots,\vec{p}_A\},\ \vec{r}_1 = \vec{r}_1(t,\omega),\ldots,\vec{p}_A = \vec{p}_A(t,\omega) \quad , \quad (2.5)$$

with obvious physical meaning. The variable ω simply corresponds to the different runs. The ensemble average allows to build the one-body, two-body,... A-body distribution functions from the quantities (2.5), by the following relations :

$$f_1(\vec{r},\vec{p},t) = N_\omega^{-1} \sum_\omega \sum_{i=1} \delta(\vec{r} - \vec{r}_i)\ \delta(\vec{p} - \vec{p}_i) \qquad (2.6)$$

$$f_2(\vec{r}\ ,\vec{p}\ ,\vec{r}',\vec{p}',t) = N_\omega^{-1} \sum_\omega \sum_{i\neq j} \delta(\vec{r}-\vec{r}_i)\delta(\vec{r}'-\vec{r}_j)\delta(\vec{p}-\vec{p}_i)\delta(\vec{p}'-\vec{p}_j) \qquad (2.7)$$

$$f_A(\vec{r},\vec{p},\ldots,\vec{r}^{(A)},\vec{p}^{(A)},t) = N_\omega^{-1} \sum_\omega \sum_{i_1} \sum_{i_2\neq i_1} \cdots$$

$$\delta(\vec{r}-\vec{r}_{i_1})\ldots\delta(\vec{r}^{(A)}-\vec{r}_{i_A})\ \delta(\vec{p}-\vec{r}_{i_1})\ldots\delta(\vec{p}^{(A)}-\vec{p}_{i_A}) \quad . \qquad (2.8)$$

N_ω is the number of runs. In practice, the δ-functions are replaced by step functions defined on a mesh in phase space. Although the number of runs required for a sufficient accuracy becomes rapidly prohibitive with the order of the distribution function, the INC model is potentially a theory for the evolution of the system in the one-body, two-body, ... and A-body phase spaces. It is thus potentially suited to the prediction of the ν-body observables with arbitrary ν.

Its predictive power encompasses even non observable quantities, like instantaneous baryon density.

In conclusion, the INC model is a model based on simulation, which pictures the nucleus-nucleus collision process as a succession of well-separated (in space-time) binary on-shell collisions (plus subsequent decays) proceeding as in free space. It is not embodied by mathematical equations, and therefore its relation with general theory is rather obscure (see, however, Section 4). Its dynamical content is simply and almost uniquely described by the underlined terms above. Besides these basic assumptions, it can be considered as a zero parameter microscopic model.

3. RESULTS AND PHYSICAL IMPLICATIONS

In this section we review the most important results obtained in the frame of the INC model and we discuss their physical implications, especially in relation with the reaction mechanism. We will first concentrate on the proton spectra, then examine the evolution of the system in phase space and finally discuss the production of particles.

3.1. Proton cross sections

The invariant nucleon production cross section is related to the one-body distribution function by

$$E\frac{d^3\sigma}{dp^3} = \lim_{t\to\infty}\int_0^{b_{max}} 2\pi\, b\, db \int d^3r\, E\, f_1(\vec{r},\vec{p},b,t) \quad , \qquad (3.1)$$

where we have introduced explicitly the impact parameter b dependence of f_1. The $t \to \infty$ limit is in fact not necessary, since the last integral is a constant when the collisions have ceased. The remarkable feature of the proton spectra is the exponential fall-off observed in the 90°-c.m. spectra

for dynamical systems. It tends to indicate a randomization of the nucleon motion, a property often referred to as the formation of a fireball. The randomization, however, is not complete as witnessed by the shouldering of the spectra at low energy, even at 90° in the c.m., [12]) and by the anisotropy of the angular distribution (Fig. 2).

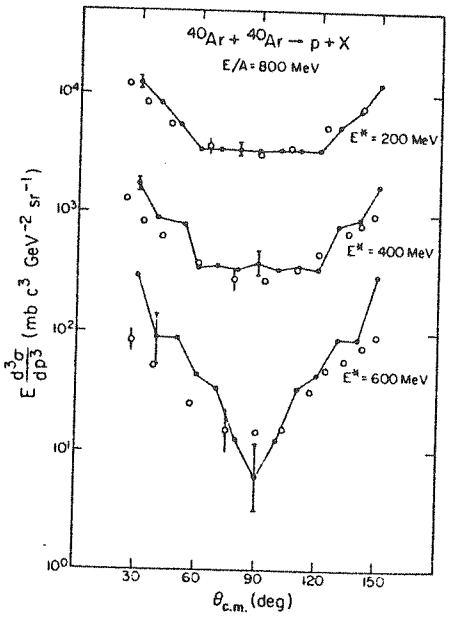

Figure 2

Invariant inclusive proton cross section as a function of the c.m. angle for the $^{40}Ar + ^{40}Ar$ system at 800 MeV per nucleon (ref.7).

This anisotropy, which is reproduced by the INC calculation, tells that the ejected protons keep some memory of the initial longitudinal motion. A clarification of this effect, as provided by the INC, is based on the examination of the momenta of the outgoing protons as a function of the number n of collisions which they have undergone. [13]) The calculated proton cross-section may be decomposed as

$$E\frac{d^3\sigma}{dp^3} = \sum_{n\geq 1}\sigma_n\, f_n(\vec{p}) = \sum_{n\geq 1} E\,\frac{d^3\sigma_n}{dp^3} \quad , \qquad (3.2)$$

where σ_n is the cross section for producing a proton having

collided n times, and $f_n(\vec{p})$ is the corresponding normalized spectrum.

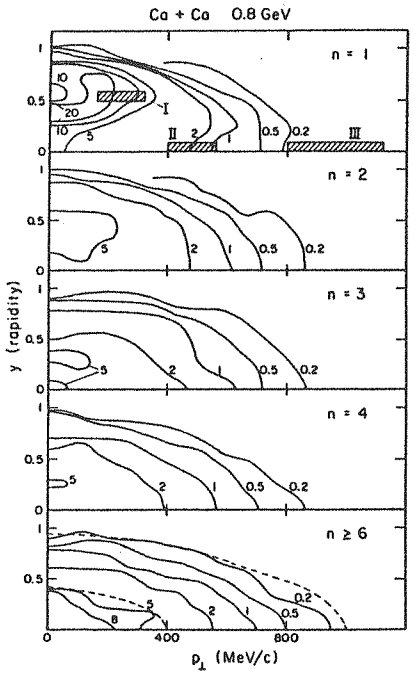

Figure 3

Contour plots ot the invariant cross sections to produce a proton having collided n times, as a function of the transverse momentum and the c.m. rapidity y. The dotted curves in the bottom correspond to isotropic emission at a definite proton energy. The system being symmetric, only half the rapidity axis is shown. (ref.13)

The different components of (3.2) are illustrated in Fig. 3 which shows the contours of constant differential cross sections in the ($p_\perp$, y) ($p_\perp$ = perpendicular momentum, y = rapidity) plane, for the Ca + Ca case at 800 MeV per nucleon. For n = 1, the proton distribution is highly unisotropic and results from the folding of the initial Fermi distribution with the nucleon-nucleon angular distribution, which at that beam energy is already rather much forward peaked. As n increases, this momentum distribution gets progressively distorted and becomes fairly isotropic (and thermalized) for $n \geq 6$.

The frequency distribution for the collision number, which governs the partial cross sections σ_n, is shown in Fig. 4.

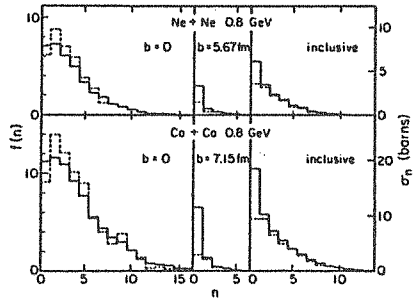

Figure 4.

Probability distribution for the number n of collisions which the particles have undergone. The full lines refer to the nucleons and the dotted lines to the Δ's. The normalization if $\sum_n f(n) = \nu$, the number of participants, for the nucleons and $\sum_n f(n) = 8\ \nu_\Delta$ for the Δ's Left : zero impact parameter Center : large impact parameter. Right : average over all impact parameters. (ref.13)

There exists, as expected, a strong difference between central and peripheral collisions. The inclusive (i.e. integrated over b) frequencies show a rather broad distribution, with a mean value of 3.24 (for Ca + Ca), which explains that randomization is - grossly speaking - reached. However total randomization is prevented by the large occurrence of small n events, especially n = 1. The trend to total randomization is favoured for larger systems, but the shape of the frequency distribution would probably prohibit total thermalization.

The large value of the cross section σ_1 suggests that a sizeable fraction of the nucleons will exit with the kinematics of the nucleon-nucleon system at the same energy. In other words, two-proton correlation yields are expected to show an enhancement in the two-nucleon kinematical region, i.e., when the two nucleons are detected in opposite directions in the c.m. system. This actually happens, as has been illustrated by the experiments of Nagamiya et al. [14]). They will not be discussed here in detail ; the

extraction of the importance of the quasi-free scattering is a complicated matter indeed, but these experiments clearly demonstrate their importance.

The value of the average collision number <n> for Ca + Ca can be translated in a mean free path $\lambda \approx 2.5$ fm, but this value can only be taken as indicative as the conditions (density, f.i.) are very much changing during the collision process. It is however interesting to note that this value is consistent with the one extracted from the correlation experiments.

3.2. Phase space evolution

The inclusive proton cross section is the simplest observational quantity associated with the dynamical evolution of the system, but constitutes only a small piece of the information contained in the one-body distribution function, as is evident from eq. (3.1). We will discuss this point now in more detail.

3.2.1. Density evolution

Matter density is related to the one-body distribution function by

$$\rho(\vec{r},t) = \int d^3p \; f_1(\vec{r},\vec{p},t) \quad . \tag{3.3}$$

We will successively look at the salient features of this function for (almost) peripheral and for central collisions.

A) Peripheral collisions

A remarkable success of the INC calculations is the theoretical support of the participant-spectator picture [15]. According to it the longitudinal translation entails a geometrical division of the system into two cold pieces of

nuclear matter (spectators) and a central highly excited part (the participants). This scheme roughly corresponds to the density plot of fig. 5, which shows the density in the reaction plane of the Ca + Ar collision at 1 GeV per nucleon, with an intermediate impact parameter [16].

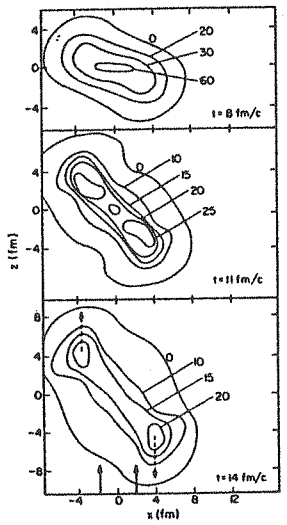

Figure 5.

$^{40}Ca + {}^{40}Ca$, b = 3.83 fm, E_{beam} = 1 GeV. Contour plot of the density in the reaction plane. The arrows at the bottom of the figure give the geometrical cut between spectator and participant matter. The dotted arrows indicate the general motion of the spectator parts. The density is given in 1/18 ρ_0 units.

In ref. [16], such a contour plot has been analysed to extract the number of participants, or more precisely the number of nucleons in the central region. The result comes close to the value predicted by the clean-cut geometrical picture, but it is a little lower, for all impact parameter ; this indicates a small, but finite transparency of the nuclear matter.

The division of the system in three pieces, with a cold fragment travelling with the velocity of the beam, has strong influence on the pion yield in the forward region. Negative pions emitted with the velocity of the beam are strongly focused in contradistinction with the positive pions which are repelled by the positive charge of the cold fragment. Time evolution of the charge distribution as

calculated with the INC model is producing a Coulomb distortion in agreement with the π^-/π^+ yield measurement [17], as it has been shown in ref. [16].

B) Central collisions

Detailed account of the baryon density distribution has been given in the early publications [8,11,18]. We give here a simplified presentation, which, however, retains the main features. As can be seen from figs. 6 and 7, the collision process can be divided into two stages : a compression stage and an expansion stage. The top of figs. 6-7 shows that the compression is largely longitudinal and at the end of the compression stage (i.e., ~ 8 fm/c in this case), the system has a pancake shape. The transformation of the longitudinal motion into a random motion takes longer ; as time proceeds, the shape of the system becomes more and more spherical during the expansion stage.

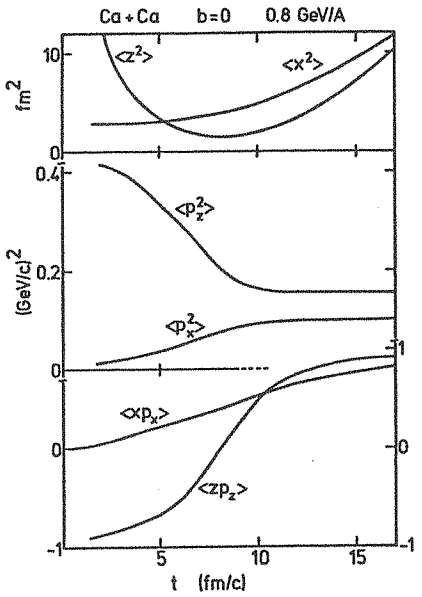

Figure 6.

Time evolution of various moments of the one-particle distribution function f_1. The non diagonal moments $\langle xp_x \rangle$ and $\langle zp_z \rangle$ have been normalized by dividing by $(\langle x^2 \rangle \langle p_x^2 \rangle)^{\frac{1}{2}}$ and $(\langle z^2 \rangle \langle p_z^2 \rangle)^{\frac{1}{2}}$, respectively. z stands along the beam axis.

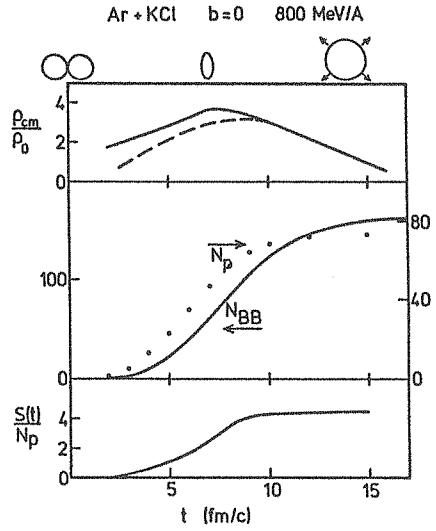

Figure 7.

Time evolution of the baryon density (dashed line : participants only, full line : all baryons included) normalized to the normal density of nuclear matter (top), of the number of baryon-baryon collisions (centre, scale on the left), of the number of participants (centre, scale on the right), and of the entropy of the participants system divided by the final number of participants (bottom).

3.2.2. Momentum distribution evolution

For E/A $\gtrsim$ 1 GeV, this evolution is governed in the early stages of the nuclear collision by two mechanisms whose consequence is sketched in fig. 8 (where, for simplicity, Fermi motion is neglected) : the elastic scatterings entail a motion along the kinematical circle ; on the other hand the inelastic interaction (Δ production) brings the nucleons close to rest in the c.m. Subsequent collisions of course lead to a more uniform population. The net result for the moments of the momentum distribu-

tion is given in fig. 6. As already noticed, the randomization is not complete. It should be noted, however, that a fraction of the incident energy has been transferred to the pions.

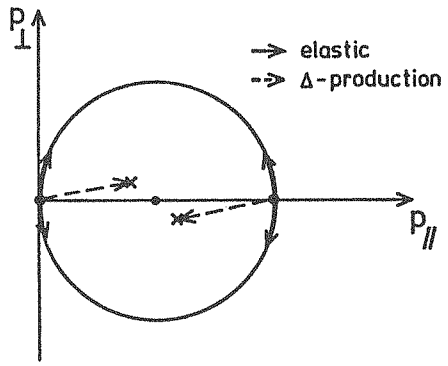

Figure 8.

Schematic evolution in momentum space for the early times of the collision. (See text).

3.2.3. Phase space occupancy and entropy

The evolution of the system reveals interesting and complicated features when a global look at phase space is taken. Figure 7 shows that the system (more precisely the participants in the system) gains entropy during the compression stage. We recall that the entropy per baryon is related to the one-particle distribution function by

$$\frac{S}{A} = 1 - A^{-1} \int d^3r\, d^3p\, f_1(\vec{r},\vec{p},t)\, \ell n\, [f_1(\vec{r},\vec{p},t)(2\pi\hbar)^3] + 4\, \ell n\, 2 \qquad (3.4)$$

or, roughly, by

$$\frac{S}{A} \approx 1 - \ell n\, [\bar{f}_1(2\pi\hbar)^3] + 4\, \ell n\, 2 \qquad (3.5)$$

if the distribution function is sufficiently close to a constant over the available phase space. The bracket is

in some sense the average number of nucleons per natural unit in phase space. After t ≈ 8 fm/c, the system expands at constant entropy. The gain in entropy from configuration space is compensated in momentum space. But this compensation lasts a small time span . After 10-11 fm/c, the system is still expanding, but the momentum distribution does not change anymore (see fig. 6). We face then a free expansion characterized by a strong correlation between position and momentum. In fact, the behaviour of the xp_x and zp_z correlations allows to consider the system as a more or less equilibrated system, i.e. with little correlations, during a very short time interval, say from 7 to 9 fm/c.

Let us notice before closing this section, that entropy of the order 4.4 as calculated by the INC calculation corresponds to a fermion occupancy in phase space of the order 1/10 per unit volume, which justifies a posteriori the neglect of the Pauli principle. We will come back to the entropy when discussing deuteron production.

3.3. Particle production

We successively discuss (briefly) the production of pions and of positive kaons and the emission of deuterons, all processes which have raised interesting questions.

3.3.1. Pions

The observable of interest, which has been under active investigation, is the (negative) pion multiplicity in central symmetric collisions (fig. 9). Originally, this quantity was believed to be strongly influenced by the behaviour of Δ-particles inside nuclear matter, which serve as catalysts in the transformation of the energy of the incoming nucleons into pions. However, it turned out that none of the reasonable models for the Δ-propagation in INC models can provide

a satisfactory account of the π yield. If the Δ's are given a long lifetime (to stimulate possible dense matter effect), the predicted yield is close to the observed one, but the π spectra are badly reproduced [8]). This comes essentially from the fact that slow Δ's in the c.m. cannot generate slow pions in the same system. On the other hand, if the Δ's are given their natural lifetime (the pion yield is rather insensitive to other quantities relative to the Δ's), the shape of the calculated pion spectra comes out rather good, but the pion yield is overpredicted, especially in the vicinity of the effective threshold.

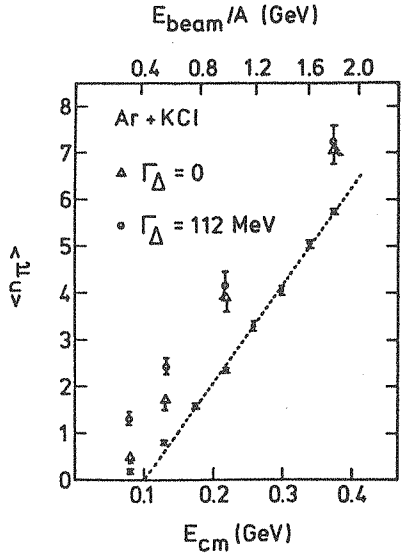

Figure 9.

The negative pion yield measured by a central trigger for Ar + KCl collisions (data around the dotted line) is compared to the prediction of INC (open circles). The triangles are the results obtained in a calculation with frozen Δ-isobars.

This discrepancy has been exploited in ref. [19]) to extract information on the nuclear equation of state. The idea is that at the end of the compression stage, some energy is stored in the compression energy and is not available to produce pions. This remark, conjugated with the observation (from INC results) that the pion multiplicity is already fixed at the end of the compression stage leads

to the relations

$$\langle n_\pi \rangle_{exp} = f(E_o - E_c(\bar{\rho}), \bar{\rho}) \qquad (3.6)$$

and

$$\langle n_\pi \rangle_{INC} = f(E_o, \bar{\rho}) \qquad (3.7)$$

In these relations, the function f is unknown, but is characteristic of INC (and probably of any kinetic) model, E_o is the available energy (for the participants) and $\bar{\rho}$ is the average density at the maximum compression. Equations (3.6)-(3.7) can be combined to

$$\langle n_\pi \rangle_{exp} = \langle n_\pi \rangle_{INC}(E_o - E_c(\bar{\rho}), \bar{\rho}) \qquad (3.8)$$

which enables to extract $E_c(\bar{\rho})$. The analysis of ref. [19]), which heavily relies on the INC model has been very much disputed. It must be pointed out, however, that Harris and Stock [20]) have recently recast the analysis and put it on a firmer basis ; the extracted compression energy is the same as before.

Another interpretation of the discrepancy appearing in Fig. 9 will be presented in Section 4.

3.3.2. K^+ production

Positive kaons can be produced only during the early stages of the collision since, being produced in association with hyperons - they require much energy. Afterwards they are not destroyed since they are only scattered elastically by nucleons. For these reasons, they are believed to carry over some information from the very hot and compressed phase formed by a rapid thermalization of the system, if this phase really takes place.

It is indeed true that K^+ spectra reveal a "temperature" larger than the one of nucleons or pions. To under-

stand better this situation, a calculation based on the INC has been made recently to obtain predictions for the K^+ yield and spectra [21]. Thanks to the smallness of the elementary K^+ production cross sections (like $NN \to N\Lambda K$) a perturbation scheme can be used and the invariant cross section for K^+ production in the nuclear process is written :

$$E_K \frac{d^3\sigma}{dp_K^3} = \int 2\pi b\, db \int \frac{d^3p_N}{E_N} \frac{d^3p_N'}{E_N'} \frac{1}{\sigma^{tot}_{NN'}} f(p_N, p_{N'}) \; E_K \frac{d^3\sigma}{dp_K^3} (p_N + p_{N'} \to p_{K^+} \ldots) \qquad (3.9)$$

where $f(p_N, p_{N'})$ is the (impact parameter dependent) frequency of a collision between two nucleons with 4-momentum p_N and $p_{N'}$. Formula (3.9) allows to obtain the cross section for a rare event once the sampling of the function $f(p_N, p_{N'})$ is made, by an INC calculation.

The following results are obtained : the total observed K^+ yield is correctly given by the INC model ; the K^+ spectra are consistent with the assumed mechanism, i.e. production through energetic NN collisions without reference to a hot thermalized phase, provided that a rescattering of the K^+'s is taken into account. Indeed, the rescattering of the (relatively light) kaons by still energetic nucleons broadens the spectra and taking this effect into account is necessary to reach a reasonable agreement with the data, as shown on fig. 10. Another source of K^+ production is provided by the $\pi N \to YK$ reactions which in this case contribute to about 20 % of the total K^+ yield.

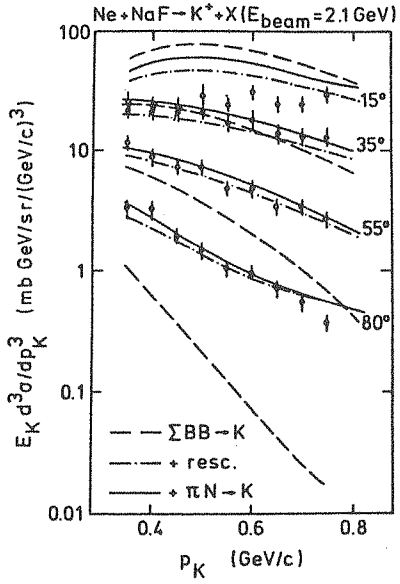

Figure 10.

Comparison between the experimental K^+ production cross section[28] and INC calculationf of ref.[21]. The dashed curves correspond to the primordial K^+ production through baryon-baryon collisions. The dot-and-dashed curve is obtained by applying a correction due to the rescattering of the kaons. The full curve includes the contribution of the $\pi N \to YK$ channels.

3.3.3. Deuteron production

The INC model is basically a gas dynamical model neglecting interactions, except for their ability to change the momenta of the particles in close encounters. The interactions can also change the nature of a baryon or induce the creation (or annihilation) of a meson but, strictly speaking, no ingredient of the INC model mentioned so far can induce the formation of composite particles. However, the formation of deuterons may be imagined as a residual

effect of the nucleon-nucleon interaction which binds a neutron and a proton together when their correlation in phase space is similar to the one existing in the deuteron system. This is translated into a formula giving the deuteron production cross section in the form :

$$E\,\frac{d^3\sigma}{dP^3} = \int d^3R\; E\; f_d(\vec{R},\vec{P}) \qquad (3.10)$$

where

$$f_d(\vec{R},\vec{P}) = \frac{3}{4}\int d^3r\,d^3p\; f_2^{np}\left(\vec{R}+\frac{\vec{r}}{2},\ \frac{\vec{P}}{2}+\vec{p},\ \vec{R}-\frac{\vec{r}}{2},\ \frac{\vec{P}}{2}-\vec{p}\right)\, g_d(\vec{r},\vec{p}) \quad . \qquad (3.11)$$

In this equation, f_2^{np} is the two-particle distribution function f_2 (see eq. (2. 7)), specialized to the neutron-proton pair and $g_d(\vec{r},\vec{p})$ is the distribution function of the relative distance and momentum in the deuteron, normalized to unity. The set (3.10)-(3.11) embodies a generalized version of the coalescence model, which states that a deuteron is formed merely because a neutron and a proton are close to each other in phase space ; the coalescence formula is retrieved by assuming that $f_2 \approx f_1\, f_1$ and that g_d is peaked around $\vec{r} = \vec{p} = 0$. It should be noted, however, as has been stressed in refs. [22,23]), that (3.10)-(3.11) corresponds to the existence of correlations like in the deuterium but that the occurence of such correlations inside heavier composites is not excluded. Therefore (3.10) is the cross section for the emission of what is now called a deuteron-like object ("d"). Assuming the n-p correlations roughly the same in any light composite, it can be estimated how many "d"'s are present in ^{3}H, ^{3}He, ... nuclei [22]). For instance, counting clusters up to ^{4}He, one has

$$\sigma_{"d"} = \sigma_d + \frac{3}{2}\,(\sigma_{^3\mathrm{H}} + \sigma_{^3\mathrm{He}}) + 3\,\sigma_{^4\mathrm{He}} \quad . \qquad (3.12)$$

In ref. [22]), eq. (3.10) is applied at the end of the collision process, whereas in ref. [23]) it is applied once every nucleon of the pair has interacted for the last time.

The results of such a calculation are given in fig. 11 for the Ne + U system at 400 MeV/A. The agreement with experiment is rather satisfactory. It can be seen that deuteron emission is more forward peaked than proton emission.

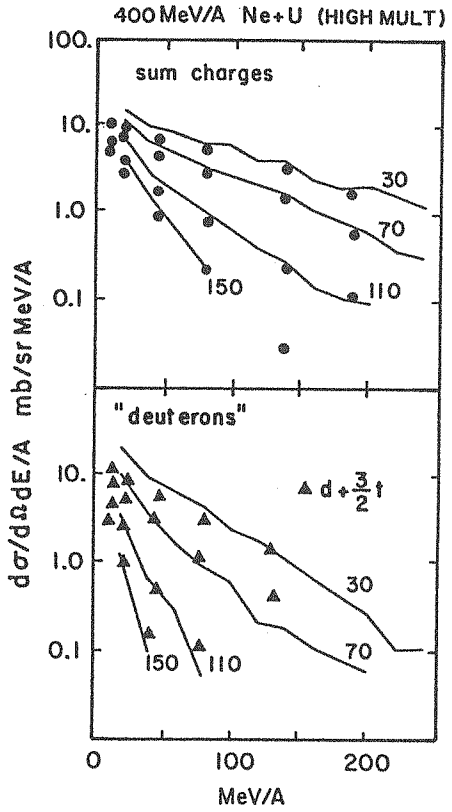

Figure 11.

INC predictions of ref. [23]) of proton-like and deuteron-like cross section in the Ne + U system at 400 MeV/A. Experimental data are represented by dots and triangles. The numbers represent the angles (in degrees) in the lab. system.

The deuteron yield can be related to the entropy, as shown for the first time by Siemens and Kapusta [24]). We

follow here the presentation of ref. [22]). The number of "d"'s is given by :

$$N_{"d"} = \frac{3}{4} \int d^3R d^3P \int d^3r d^3p \; f_2^{np}(\vec{R}+\frac{\vec{r}}{2}, \frac{\vec{P}}{2}+\vec{p}, \vec{R}-\frac{\vec{r}}{2}, \frac{\vec{P}}{2}-\vec{p}) \; g_d(\vec{r},\vec{p}) \; . \tag{3.13}$$

If we assume that the function g_d is very narrow, and if we neglect np correlations in f_2^{np}, we have (for a symmetric N = Z system)

$$N_{"d"} = \frac{3}{16} \int d^3R \; d^3P \; (f_1(\vec{R},\frac{\vec{P}}{2}))^2 = \frac{3}{2} \langle f_1 \rangle \int d^3R \; d^3P \; f_1(R,P) \quad , \tag{3.14}$$

where $\langle f_1 \rangle$ is the average of f_1 over its own distribution. The last integral in eq. (3.14) is twice the proton number. Once again, not only free protons should be counted, but also the protons contained in the composites. Let us denote these objects by "p". One readily gets

$$\langle f_1 \rangle = \frac{1}{3} \frac{N_{"d"}}{N_{"p"}} \quad . \tag{3.15}$$

Now, eq. (3.4) gives

$$\frac{S}{A} = 1 - \langle \ell n \; f_1 \rangle + 4 \; \ell n \; 2 \; . \tag{3.16}$$

Using a thermal model (which may not be correct) allows to relate $\langle \ell n \; f_1 \rangle$ to $\ell n \langle f_1 \rangle$ [25]). The final result is

$$\frac{S}{A} = \frac{5}{2} + \frac{1}{2} \; \ell n \; 2 - \ell n \langle f_1 \rangle \quad , \tag{3.17}$$

or, using (3.15) and introducing numerical values :

$$\frac{S}{A} = 3.95 - \ell n \frac{N_{"d"}}{N_{"p"}} \quad , \tag{3.18}$$

which has the same structure as the formula of ref. [24]). However, the deuterons and protons have been replaced by deuteron-like and proton-like objects.

Originally, the integrated cross sections were used in connection with eq. (3.18) to extract from experiment the entropy produced. The value was larger than the value

calculated for central collisions with the INC model. However, it was realized afterwards [9,26]) that there is a strong impact parameter dependence of the entropy per baryon, as is shown in fig. 12. This pattern suggests a long mean free path (a few fm). Later on, experimentalists have demonstrated a dependence on charged multiplicity, which is very similar to the one of fig. 12 : for large multiplicities the entropy is lower and seems to saturate. In fig.13 we compare the saturation values for various systems with the estimate of ref. [27]), using the INC model. The agreement is quite good. We must say however that a small deviation in S/A gives rise to a larger deviation in the ratio $N_{"d"}/N_{"p"}$ because of the logarithmic relationship.

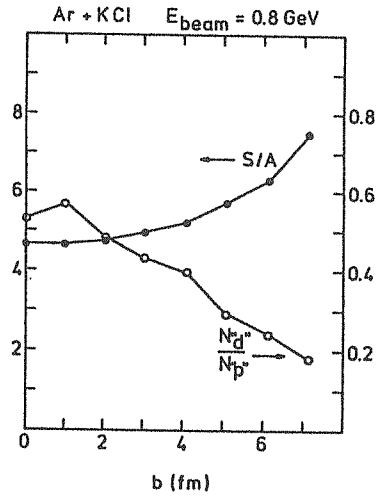

Figure 12.

INC calculation of the entropy per baryon and the deuteron proton ratio as a function of impact parameter.

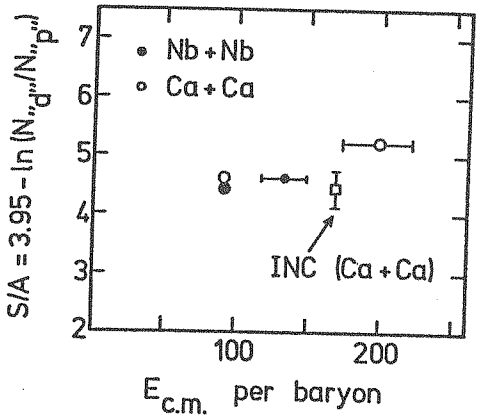

Figure 13.

Experimental values [27]) of the "d"/"p" ratio (or the entropy) for large multiplicities compared to the INC calculations of ref. [22]). See text.

4. THEORETICAL BASIS. EXTENSIONS

There is a widely spread opinion that the INC calculations are essentially a numerical trick to solve the Boltzmann equation for dilute gases. In this section, we critically examine this matter as well as its connection to the general kinetic theory.

4.1. The Boltzmann equation

This equation is an evolution equation for the one-body distribution function. For the sake of simplicity, we present here a non relativistic version for a single fluid. In the practical case of heavy ion reactions, one should generalize to coupled equations for the one-body distribution functions of the different species. The equation can be written (in the absence of external field) as

$$\left(\frac{\partial}{\partial t} + \frac{\vec{p}}{m}\cdot\vec{\nabla}\right) f_1(\vec{r},\vec{p},t) = G - L \quad , \tag{4.1}$$

where the gain term G and loss term L have been derived by Boltzmann by analyzing the effects of two-body collisions. The loss term has a straightforward structure

$$L = f_1(\vec{r},\vec{p},t) \int d^3p' \, \frac{|\vec{p}-\vec{p}'|}{m} \, \sigma \, f_1(\vec{r},\vec{p},t) \quad , \tag{4.2}$$

where σ is the total collision cross section. The gain term can be written as

$$G = \int d^3p_1 \int d^3p_1' \; f_1(\vec{r},\vec{p}_1,t)\, f_1(\vec{r},\vec{p}_1',t)\, \sigma \, \frac{|\vec{p}_1-\vec{p}_1'|}{m} \, \delta(\vec{p}_{out}-\vec{p}) \tag{4.3}$$

The delta function restricts to collisions which can produce an outgoing particle with momentum $\vec{p}$. It can be shown that eq. (4.3) can be put in the form [29]

$$G = \int d^3p' \int d\Omega \, \frac{|\vec{p}-\vec{p}'|}{m} \left(\frac{d\sigma}{d\Omega}\right) f_1(\vec{r},\vec{p}_1,t)\, f_1(\vec{r},\vec{p}_1',t) \quad , \tag{4.4}$$

where $\vec{p}_1$ and $\vec{p}_1'$ are now restricted by the conservation laws

$$\vec{p} + \vec{p}' = \vec{p}_1 + \vec{p}_1' \quad , \tag{4.5a}$$

$$p^2 + p'^2 = p_1^2 + p_1'^2 \quad . \tag{4.5b}$$

When the direction $\Omega = (\vartheta,\varphi)$ of $\vec{p}_1$ respective to $\vec{p}$ in the c.m. system is specified, the vectors $\vec{p}_1$, $\vec{p}_1'$ are uniquely determined.

The Boltzmann equation is (as the INC) a scheme which stands "half-way between a phenomenological stochastic theory and a rigourous dynamical theory", following the author of ref. [29]). A rigourous dynamical theory at the classical level exists, although it is not tractable at all : it is usually denoted in the literature under the name of Bogolioubov-Born-Green-Kirkwood-Yvon (BBGKY) theory [30]) (a quantum counterpart also exists). It starts from the Liouville equation for the full distribution function and successive equations for the one-body, two-body, ..., ν-body distribution functions are obtained by integrating over the coordinates of A-1, A-2, ..., A-ν particles. The first equations write

$$\left[\frac{\partial}{\partial t} - L_o(1)\right] f_1 = \int d^3r_2 \, d^3p_2 \, L_{12}' \, f_2(\vec{r}_1,\vec{p}_1,\vec{r}_2,\vec{p}_2,t) \tag{4.6}$$

$$\left[\frac{\partial}{\partial t} - L_o(1) - L_o(2)\right] f_2 = L_{12}' \, f_2(\vec{r}_1,\vec{p}_1,\vec{r}_2,\vec{p}_2,t) + \int d^3r_3 \, d^3p_3 (L_{13}' + L_{23}') \, f_3(\vec{r}_1,\vec{p}_1,\vec{r}_2,\vec{p}_2,\vec{r}_3,\vec{p}_3,t) \tag{4.7}$$

with

$$L_o(i) = \frac{\partial H}{\partial \vec{r}_i} \cdot \frac{\partial}{\partial \vec{p}_i} - \frac{\partial H}{\partial \vec{p}_i} \frac{\partial}{\partial \vec{r}_i} \tag{4.8}$$

and

$$L'_{12} = [\vec{\nabla}_1 V(\vec{r}_1 - \vec{r}_2)].(\frac{\partial}{\partial \vec{p}_i} - \frac{\partial}{\partial \vec{p}_2}) \quad . \tag{4.9}$$

Here, the Hamiltonian H is assumed to be of the form

$$H = \sum_{i=1}^{A} \frac{p_i^2}{2m} + \sum_{i<j} V(\vec{r}_i - \vec{r}_j) \quad . \tag{4.10}$$

The structure of the BBGKY equations can be guessed from eqs. (4.6)-(4.7). The evolution equation for f_ν involves $f_{\nu+1}$: the equations never close on themselves (in an extended system) and they are said to form a hierarchy.

In view of these equations, the Boltzmann equation looks like an acceptable equation in the dilute limit. The argumentation goes as follows. Assume f_2 is not very different from the products of two f_1 and that the system is so dilute that an interacting pair has little chance to interact with a third partner. Then the last term in (4.7) is negligeable and formal solution of f_2 replaced in (4.6) makes appear repeated interactions between particles 1 and 2, i.e. something which has to do with the scattering matrix.

The conditions of validity of the Boltzmann equation are not a trivial matter. They are, however, established heuristically in many textbooks . We follow here ref. [29]). First of all, the basic assumption is that there exists an interval Δt such that

$$\tau_c << \Delta t << \tau_r \quad , \tag{4.11}$$

where τ_c is the (elementary) collision time and τ_r the relaxation time. This condition is easy to understand : one cannot look for variations over characteristic times which are too short since one has neglected the change in the system when the trajectories of the particles are different from a straight line. On the other hand the relaxation of the system, i.e. the evolution of strong local inhomogeneities, cannot be described by derivatives if the relaxation time is too short. The condition (4.11) is often stated as a low density condition (which may not be strictly equivalent)

$$r_c^3 \rho << 1 \quad . \tag{4.12}$$

Physically, the latter condition ensures that the successive collisions are well separated in space-time.

In deriving the Boltzmann equation, one implicitly assumes that the distribution function does not change significantly over the time interval Δt. In other words, one assumes that the Boltzmann equation is local in time or equivalently that the evolution is a Markovian process. Similarly, one also neglects space variation of the distribution function over lengths $\Delta \ell$, typical of the distance travelled by the particles during the time Δt : the equation is local in space.

Finally, the factorization

$$f_2 = f_1 f_1 \tag{4.13}$$

is required : this is the celebrated "Stosszahlansatz" or "molecular chaos" assumption, which introduces irreversibility as is well known.

From the description of the INC model, it is evident that much less stringent assumptions are required for the INC picture to be correct. Since one does not deal with time derivative, one needs not worry about a characteristic interval Δt smaller than the relaxation time. Only condition (4.12) is required. The very structure of the INC calculation is not subject to conditions on locality in space-time. Obviously, the INC model describes a non-Markovian process, since the evolution really depends upon the previous history of the system. Finally, whether a two-body collision occurs or not depends in the INC picture on the probability of finding two nucleons at sufficiently close points with an appropriate relative momentum, a quantity which has something to do with the two-body distribution function f_2 . Therefore, the two-body correlations effects are really taken into account. Three-body and higher

correlations are, of course, neglected as in the Boltzmann equation. In conclusion, the really important condition for the validity of the INC model (besides the condition of the quasi-classical motion) is the low-density condition (4.12), which, as we said in the introduction, is only marginally satisfied. On the other hand, it can be said that the INC model is a kinetic theory, which goes farther than the Boltzmann equation does, in the treatment of two-body correlations.

4.2. From the Boltzmann equation to Hydrodynamics

The Boltzmann equation possesses several important properties. We recall here two of them.

(1) The one-body entropy (contrarily to eq. (3.4), we assume here one type of particles only)

$$\frac{S}{A} = 1 - \frac{1}{A} \int d^3r\, d^3p f_1(\vec{r},\vec{p},t)\, \ell n[f_1(\vec{r},\vec{p},t)(2\pi\hbar)^3] \qquad (4.14)$$

cannot decrease.

(2) There are five (and five only) collisional invariants, i.e. quantities which are constant as the collisions proceed. They are :

$$I_n = \int d^3r\, d^3p\, \gamma_n\, f(\vec{r},\vec{p},t) \quad , \qquad (4.15)$$

with

$$\gamma_n = 1,\ p_x,\ p_y,\ p_z,\ p^2 \quad . \qquad (4.16)$$

These conservation laws may be written in a differential form governing the time evolution for the spatial densities associated with the quantities I_n . They may be obtained equivalently by considering the moments (in p) of the Boltzmann equation. The zeroth moment gives (see eqs. (4.1)-(4.2))

$$\frac{\partial}{\partial t} \int d^3p\, f_1(\vec{r},\vec{p},t) + \vec{\nabla}. \int d^3p\, \vec{p}\, f_1(\vec{r},\vec{p},t) = 0 \qquad (4.17)$$

or

$$\frac{\partial \rho}{\partial t}(\vec{r},t) + \vec{\nabla}.(\rho\, \vec{u}(\vec{r},t)) = 0 \quad , \qquad (4.18)$$

where

$$\vec{u}(\vec{r},t) = \frac{\int d^3p\, \frac{\vec{p}}{m} f_1(\vec{r},\vec{p},t)}{\int d^3p\, f_1(\vec{r},\vec{p},t)} \qquad (4.19)$$

can be interpreted as the macroscopic velocity. The first moments give

$$\frac{\partial}{\partial t}(\rho\, \vec{u}) + \vec{\nabla}. \int d^3p\, \frac{\vec{p}}{m} \frac{\vec{p}}{m} f_1 = 0 \quad , \qquad (4.20)$$

or, using the local deviation from the average velocity ($\frac{\vec{p}}{m} = \vec{u} + \vec{v}$),

$$\frac{\partial}{\partial t}(\rho\, \vec{u}) + \vec{\nabla}.\{\rho\, \vec{u}\, \vec{u} + \rho\, \vec{v}\, \vec{v}\} = 0 \quad . \qquad (4.21)$$

With the help of eq. (4.18), one readily obtains

$$\rho\{\frac{\partial u}{\partial t} + (\vec{u}.\vec{\nabla})\vec{u}\} = - \vec{\nabla}.\underset{\approx}{P} \quad , \qquad (4.22)$$

where we have introduced the usual pressure tensor

$$P_{ij} = \int d^3p\, v_i\, v_j\, f_1(\vec{r},\vec{p},t) \quad . \qquad (4.23)$$

At this stage, one can easily guess a feature of the structure of the equations for the different moments : the time derivative of the ν^{th} moment involves the $(\nu+1)^{th}$ moment. The moment equations form an infinite hierarchy.

The equation for the p^2 moment (which is the sum of three of the nine second moments) can be written, using the same techniques :

$$\rho[\frac{\partial}{\partial t} e + \vec{u}.\vec{\nabla}e] + \vec{\nabla}.\vec{J} = - \underset{\sim}{P} : \vec{\nabla}\vec{u} \quad , \tag{4.24}$$

where e is the kinetic (thermal) energy density per unit mass

$$\rho\, e(\vec{r},t) = \int d^3p \, \frac{p^2}{2m} \, f_1(\vec{r},\vec{p},t) - \frac{1}{2} \rho \, u^2 \quad , \tag{4.25}$$

and where $\vec{J}$ is the heat-flow density vector

$$\vec{J} = \int d^3p \, \frac{(\vec{p} - m\,\vec{u})^2}{2m} \, (\frac{\vec{p}}{m} - \vec{u}) \, f_1(\vec{r},\vec{p},t) \quad . \tag{4.26}$$

Once again, eq. (4.24) involves a higher moment, namely $\vec{J}$. It is worthwhile to note that the collision term in the Boltzmann equation does not contribute to these moment equations, because of the symmetry of the collisions, whereas it may (and generally does) contribute to the evolution of the entropy. Equations (4.18), (4.22), (4.24) are useless because they contain unknown quantities, namely $\underset{\sim}{P}$ and $\vec{J}$, which are determined by the solution of the Boltzmann equation itself.

In general, the hierarchy of the moment equations is closed on itself by a phenomenological procedure. Let us first remind that the collision term vanishes for $f_1(\vec{r},\vec{p},t)$ of the form

$$f_1(\vec{r},\vec{p},t) = \rho(\vec{r},t)\left(\frac{1}{2\pi\, mkT(\vec{r},t)}\right)^{\frac{3}{2}} \exp\{-\frac{(\vec{p} - m\vec{u}(\vec{r},t))^2}{2\, mkT(\vec{r},t)}\} \tag{4.27}$$

which corresponds to a local thermal equilibrium. In this case,

$$P_{ij} = p\, \delta_{ij} \quad , \quad p = \rho kT \quad , \quad \vec{J} = 0 \quad . \tag{4.28}$$

A system with such a one-body density cannot be stationary. The quantities ρ, $\vec{u}$, T will evolue because of the $\vec{p}.\vec{\nabla}\, f_1$ term (the convection term) in the l.h.s. of the Boltzmann equation, which drives particles from one point to another. Obviously, corrections to (4.28) will come from gradients

of the intensive macroscopic quantities ρ, $\vec{u}$, T. Because P is a rank-2 tensor, it should be corrected as :

$$P_{ij} = p\, \delta_{ij} - \eta(\frac{\partial u_j}{\partial x_i} + \frac{\partial u_i}{\partial x_j} - \frac{2}{3}\, \delta_{ij}\, \vec{\nabla}.\vec{u}) - \zeta\, \delta_{ij}\, \vec{\nabla}.\vec{u} \quad , \tag{4.29}$$

where η and ζ are the shear and bulk viscosity coefficient, respectively. The heat flow $\vec{J}$ should be of the form

$$\vec{J} = - \lambda\, \vec{\nabla}\, \rho - \varkappa\, \vec{\nabla}\, T \quad , \tag{4.30}$$

where $\varkappa$ is the termal conductivity. Equations (4.18), (4.22), (4.24) with expressions (4.29), (4.30) are the fundamental equations of hydrodynamics for a real fluid (i.e. with viscosity and thermal conductivity). They still contain too many unknown functions. This situation is cured by eliminating the pressure and the internal energy in terms of ρ and T. The functional relationship, called the equation of state, is assumed to be the same as in equilibrium

$$p = p(\rho,T) \tag{4.31a}$$

$$e = e(\rho,T) \quad . \tag{4.31b}$$

One thus ends with 5 scalar equations for 5 unknown functions $(\rho,\vec{u},T)$.

It should be realized that the hydrodynamical approach basically assumes a local equilibrium. Equivalently stated, it assumes that the one-body distribution function is never far from expression (4.27). This has important consequences. Consider a small cell in fluid. It may contain a small number of particles and large fluctuations may occur around (4.27). Therefore, one has to consider cells which are large enough for smearing out the fluctuations. This is realized if the linear dimension of the cell is at least as large as the mean free path of the particles. In conclusion, one may say that hydrodynamics, which averages over small distance (and small time interval) can handle long

range variations with characteristic length larger than the mean free path. On the other hand, hydrodynamics is not necessarily limited to weakly interacting systems. In other words, the equation of state may be different from that of an ideal gas.

4.3. The heavy ion case

In the heavy ion case around 1 GeV/A, the mean free path for making a collision is of the order of 1.5 fm (see fig. 1). However, what matters indeed is not the mean free path for making a collision, but the mean free path for thermalizing a particle. As we have said, the nucleon-nucleon elastic cross section is rather forward peaked in this energy range. About three collisions are required for stopping a particle. This makes the relevant mean free path of the order of 4-5 fm. Such a situation cannot be handled properly by hydrodynamics. Of course, as the nucleus-nucleus collision proceeds, the situation becomes more favourable for hydrodynamics : in the average, the nucleons have less relative kinetic energy. This has at least two consequences. In the first moments of the collision, the one-body distribution function is certainly not of the form (4.27). Secondly, nucleons close to the surface (within a mean free path) will have a high probability of leaving the system without being thermalized. As we have already said in Section 2.1, these effects have been experimentally demonstrated in systems like Ar + KCl. Moreover, two-proton correlation experiments clearly show that the two-body distribution function is not factorizable, which would happen in a (locally) thermalized system. This rather large mean free path (which shows also its effect in the b-dependence of the entropy) produces a real though limited transparency of the nuclei. In order to cope with such a situation, one-fluid calculations have been replaced by two-fluid calculations with a weak interaction between the two fluids.

In order to detect collective behaviour, as predicted by hydrodynamics, experimentalists have turned to the analysis of the collision by means of global variables. A global variable characterizes the outcome of the collision in a way which is intuitively comprehensive. It is computed event by event and for each event results from a summation over all the emitted particles (ejectiles). The simplest of the global variables is the number of ejectiles. But it is more instructive to look at quantities constructed from the momenta, as they will reflect properties of the emission pattern. We shall focus on the quantities making up the sphericity tensor

$$Q_{ij} = \sum_{\nu} \gamma_{\nu} \, p_i^{(\nu)} \, p_j^{(\nu)} \qquad (4.32)$$

where $p_i^{(\nu)}$ is the i^{th} Cartesian coordinate of the ν^{th} ejectile. The quantity γ_{ν} is a weighting factor. Generally $\gamma_{\nu} = m_{\nu}^{-1}$ or E_{ν}^{-1} . These choices are said coalescence-invariant : a deuteron or a proton and a neutron with the same velocity contribute in the same way to the sphericity tensor. The symmetric tensor Q_{ij} is better characterized by the three principal axes of the corresponding ellipsoid and by three angles. The absolute size of the tensor being simply related to conservation laws, only the ratios

$$q_1 = \frac{\lambda_1}{\lambda_3} \quad , \quad q_2 = \frac{\lambda_2}{\lambda_3} \qquad (4.33)$$

are considered. Here, λ_1, λ_2, λ_3 are the three axes ordered by decreasing sizes. If q_1 is large, the emission of ejectiles is strongly focused. On the other hand, if $q_1 \approx 1$ (with also $q_2 \approx 1$), the emission is largely isotropic. Generally, only the angle Φ, which is the polar angle of the largest axis with respect to the beam axis is considered.

Figure 14 shows the frequency of events as a function of the ratio q_1 and the angle Φ for "central trigger" Ca + Ca collisions. As one can see the cascade calculation

of ref. [31]) gives a good reproduction of the data, whereas hydrodynamics predicts a much more sideward emission resulting from the incompressibility of nuclear matter. In the average, as explained in ref. [31]), the large axis of the ellipsoid points towards 0°, but since the polar angle only is measurable, its average value appears at ~ 20°, which merely reflects the fluctuations from event to event. In ref. [32]), techniques are provided to get rid of this effect. In the recent Nb + Nb data [33]), the situation seems to indicate a sidewards collective flow after the collision, which is beyond the possibility of the standard INC code of Yariv and Frankel.

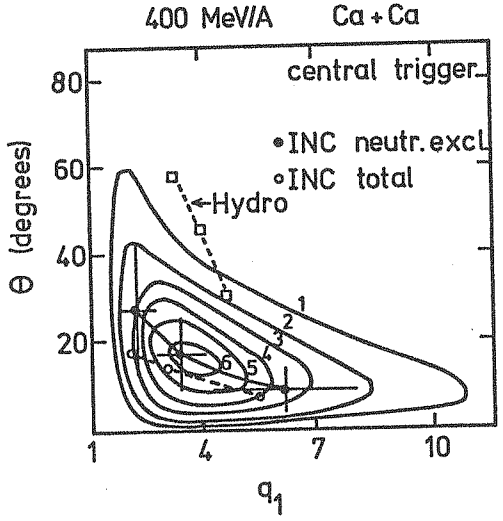

Figure 14.

Contours of the experimental frequency of events with parameters q_1, ϑ of the sphericity tensor (see text) for Ca + Ca collisions measured with the central trigger of the plastic ball and predictions of intranuclear cascade calculations [31]) and of the hydrodynamical calculations [34]). The full dots refer to charged particles only. For each calculation (INC : dots, Hydro : squares), the symbols correspond (from left to right) to b = 0, 2, 4 fm, respectively. The error bars indicate the fluctuations as predicted by the INC calculations (rms deviations).

In conclusion, the INC model is able to describe non-equilibrium situations which leave important tracks in experimental data. If the collision time is large enough, the INC exhibits collective (hydrodynamical) patterns, which are increasing with the size of the system, but which are smaller than those encountered in a pure hydrodynamical approach.

4.4. Improvements of the INC model

There are many points on which the INC model can be improved. Many of them (Pauli principle, relativistic invariance, 2π production, etc...) seem, according to us, more or less technical points, which do not change the basic physics significantly. However, here follow two features which may become important in the low-energy and high-energy ranges, respectively.

4.4.1. The average field

In nuclear physics, like in many systems, the particles are interacting through a potential composed of a short-range strong part, which is responsible for the high momentum transfer suffered by the colliding particles, and of a long-range part, with a weaker intensity. In the high-energy regime where the characteristic initial relative momentum is larger than the characteristic transfer momentum, the specific effect of the long-range part is neglected : that is the basic premise of the INC model. At lower energy, this is no longer justified. The specific effect of the long-range part is that particles interact (softly) with several particles at the same time. This is conveniently represented by the introduction of an average potential well, which is commonly represented as :

$$U(\vec{r},t) = \int d^3r'\, d^3p\, v_\ell(|\vec{r}-\vec{r}'|) f_1(\vec{r}',\vec{p},t) \approx 4\pi\rho \int_0^\infty v_\ell(r) r^2 dr \quad . \tag{4.34}$$

This modifies the Boltzmann equation in

$$[\frac{\partial}{\partial t} + \frac{\vec{p}}{m}.\vec{\nabla} - (\vec{\nabla} U(\vec{r},t)).\vec{\nabla}_{\vec{p}}] f(\vec{r},\vec{p},t) = G - L \quad , \qquad (4.35)$$

i.e. a Landau-Vlassov type equation. Incidentally, we mention that all the considerations made in Section 4.2 are still valid, provided in (4.28) the pressure is now replaced by

$$p = \rho kT + 2\pi \rho^2 \int_0^\infty v_\ell(r)\, r^2 dr \quad . \qquad (4.36)$$

Similarly, one now has

$$e = \frac{3}{2} \rho kT + 4\pi \rho^2 \int_0^\infty v_\ell(r) r^2 dr \quad . \qquad (4.37)$$

The problem is far from being settled, however. First of all, it is not clear in nuclear physics how to make a clear separation between the short-range and long-range part (strictly speaking, one should calculate modified cross sections associated with the short-range part only). Second, the average potential may have a momentum (or energy) dependence. Third, particles are no longer on their mass shell, i.e. the energy-momentum relation is changed. Four, the proper choice of the average potential is not obvious. One may think to calculate it from the last expression in (4.34) or start with a more empirical point of view, using an average potential which simulates the binding energy in nucleus in the initial state.

Solving the Landau-Vlassov equation appears as a hard task, similar in difficulty to solving the so-called "equations of motion" [35,36]. One may think to the problem in an iterative way. First make an INC model, then calculate the average potential, afterwards remake a new INC model, by putting the particles off their energy shell by the potential. Recalculate the average potential, etc... Whatever the details, the average potential present in the initial state will certainly be destroyed at the end of the nucleus-nucleus collisions (at least for central collisions). Residual effects may be thought to be responsible for composite production.

The first simplified step towards the study of the average potential has been done in ref. [37]. A quasi-particle picture, with particles off their mass shell, has been adopted. This is treated in a simple way by introducing either a scalar or a vector potential representing an average binding field uniform over the whole nucleus ; in the latter case, the energy momentum relativistic relation is

$$(E - V_v)^2 = \vec{p}^2 + m^2 \quad . \qquad (4.38)$$

Two extreme cases have been considered :

(a) the field survives the collision process, so that the particles remain off the energy shell all the time ;

(b) once a particle has made a collision it does not experience the binding any more.

Case (a) certainly overestimates the role of the binding. Case (b), on the contrary, probably corresponds to the highest possible rate of destruction of the field but it is not an unreasonable assumption since collisions scatter nucleons in momentum space.

To calculate the off shell cross sections it is assumed that their behaviour is governed dominantly by the available phase space for the final particles. (The effect is thus expected to be the largest close to the N + Δ threshold). The same attractive potential (V = - 40 MeV) has been taken for N and Δ, for simplicity, the pions being produced on their mass shell. As for pion production, the results in case (a) are very close to the case without potential ; this is not surprising in view of the assumption made for the cross section. In case (b) the pion yield is lowered quite significantly ; it now comes almost in agreement with experiment. Such a scheme provides an alternative explanation of the pion yield in central collisions (see Section 3.3.1).

4.4.2. The hard core potential

As we have seen in Section 3, the nuclear system may be quite compressed (in real space) when going up in energy. The shape of the nucleon-nucleon potential, especially its short-range repulsive part, may play a role in such a situation, and not simply through the cross section. Ref. [38]) gives quantitative indications on this effect. The effect of a hard core may be guessed in the frame of the Boltzmann equation. First, particles cannot come closer than the hard core diameter. Second, there is a shielding of particles through the proximity of a third partner. As explained in Ref. [38]), the first property gives rise to an equation of state of the Van der Waals type through the Enskog prescription [39]). Also, it reduces roughly the collision frequency by a factor [38])

$$Y = \frac{1 - \frac{11}{12}\,\pi\, d^3\, \rho}{1 - \frac{4\pi}{3}\, d^3\, \rho} \qquad (4.39)$$

or (with $d \approx 0.4$ fm, as in the Hamada-Johnston potential [40])

$$Y \approx \frac{1 - 0.18\,\rho}{1 - 0.27\,\rho} \quad . \qquad (4.40)$$

This effect has been detected by E.C. Halbert [41]), who used the billiard ball dynamics. Also, the maximum compression is lowered when the diameter d is increased. Although around 1 GeV/A ($\rho_{max} \approx 0.6$ fm^{-3}) the function Y is still close to unity, the effect may become more and more important as energy is increasing.

5. CONCLUSIONS

We have described the INC model as it is used in relativistic heavy ion physics. Although the various codes now available differ on technical (or sometimes less technical) points, they all implement a method to simulate the collision process as a succession of binary collisions, well separated in space-time, between free (or almost free) particles colliding with free space cross sections and sudden momentum changes. This model appears up to now as the most successful model in the GeV/A range. It has also a wide predictive power (mainly limited at present by computing time). We may give a long list of direct observables and properties : proton, pion, deuteron, K^+ cross sections, two-proton correlations, Coulomb distortion of pion spectra which are reproduced with satisfactory accuracy as well as of quantities which are derived from an analysis of the data, like the radii of the interacting zone, also in good agreement.

The INC model provides a consistent description of the different properties of the collision process ; it manages off-equilibrium and off-local-equilibrium behaviours which result from the initial stages of the collisions and from the fact that the size of the system is not very large with respect to the average mean free path. In the INC model, the concept of participant and spectator is obvious ; off-equilibrium effects are nicely interpreted in terms of the number of collisions undergone by the participants. It is expected that in a near future the INC calculations will be able to extract without too much ambiguity the size of the equilibrated part of the colliding system and derive the properties this part imprints on the experimental data.

The INC model presents a rich diversity of features : as already told, it is able to handle an off-equilibrium situation ; it may display a collective behaviour of the colliding matter if the collision time is large enough ; it can also predict fluctuations (from event to event).

This last property (already detectable in fig. 14) has not been exploited yet.

As we have indicated in Section 3, the model is not successful in every respect ; significant though small discrepancies exist for some variables. It is likely that they are linked to a necessary relaxation of the main hypotheses of the model, which are rather drastic in their simplicity. The two-body dynamics should be corrected by one-body dynamical properties, a correction expectedly more and more important as energy decreases. Ternary interactions should be more and more frequent as energy increases. Potential energy, be it compressional or else, may have a detectable influence on the observable quantities. Finally, elementary nucleon-nucleon interaction properties could be altered by the environment of the nuclear medium in collision. The modifications of the present INC along these lines, necessary to study the 100 MeV/A as well as the 10 GeV/A ranges, are still in their infancy. They are, however, eagerly waited for.

REFERENCES

1) J.R. Nix, Progress in Particle and Nuclear Physics 2 (1979) 237.
2) See ref. 1, Sect. 5, for a list of references.
3) J.N. Ginocchio, Phys. Rev. C17 (1972) 195.
4) N.J. Di Giacomo, R.M. DeVries, J.C. Peng, Phys. Rev. Lett. 45 (1980) 527.
5) Y. Yariv, Z. Fraenkel, Phys. Rev. C20 (1979) 2227, and earlier references cited therein.
6) K.K. Gudima, H. Iew, V.D. Toneev, J. Phys. G5 (1978) 229.
7) J. Cugnon, Phys. Rev. C22 (1980) 1885.
8) J. Cugnon, D. Kinet, J. Vandermeulen, Nucl. Phys. A379 (1982) 553.

9) J. Cugnon, Nucl. Phys. A387 (1982) 191c.
10) Y. Kitazoe et al., LBL-16278 preprint, 1983.
11) J. Cugnon, T. Mizutani, J. Vandermeulen, Nucl. Phys. A352 (1981) 505.
12) S. Nagamiya et al., Phys. Rev. C24 (1981) 971.
13) J. Cugnon, Phys. Rev. C23 (1981) 2094.
14) I. Tanihata et al., Phys. Lett. 100B (1981) 121.
15) G.D. Westfall et al., Phys. Rev. Lett. 37 (1976) 1202.
16) J. Cugnon, S.E. Koonin, Nucl. Phys. A355 (1981) 477.
17) W. Benenson et al., Phys. Rev. Lett. 43 (1979) 683.
18) J. Cugnon, T. Mizutani, J. Vandermeulen, Lett. Nuovo Cimento 28 (1980) 55.
19) R. Stock et al., Phys. Rev. Lett. 49 (1982) 1236.
20) J.W. Harrix, R. Stock, 7th Oaxtepec Meeting on Nuclear Physics, January 1984.
21) J. Cugnon, R.M. Lombard, Phys. Lett. 134B (1984) 392 ; to appear in Nucl. Phys. A.
22) G. Bertsch, J. Cugnon, Phys. Rev. C24 (1981) 2514.
23) M. Gyulassy, K. Frankel, E.A. Remler, Nucl. Phys. A402 (1983) 596.
24) P.J. Siemens, J.I. Kapusta, Phys. Rev. Lett. 43 (1979) 1486.
25) G. Kittel, Elementary Statistical Physics (Wiley).
26) G. Bertsch, J. Cugnon, unpublished.
27) H.H. Gutbrod et al., Intern. Topical Meeting on High Energy Nuclear Physics, Balatonfüred (June 1983).
28) S. Schnetzer et al., Phys. Rev. Lett. 49 (1982) 989.
29) R. Balescu, Equilibrium and Non Equilibrium Statistical Mechanics (Wiley-Interscience, New York, 1975), ch. 11.
30) R. Yvon, Les Corrélations et l'Entropie Statistique Classique (Dunod, Paris, 1965).
31) J. Cugnon, D. L'Hôte, Nucl. Phys. A397 (1983) 519.
32) P. Danielewicz, M. Gyulassy, Phys. Lett. 129B (1983) 283.
33) H.G. Ritter et al., Intern. Topical Meeting on High Energy Nuclear Physics, Balatonfüred, June 1983.

34) J.I. Kapusta, D. Strottman, Phys. Lett. 106B (1981) 33.
35) A.R. Bodmer, C.N. Panos, Phys. Rev. C15 (1977) 1342.
36) L. Wilets et al., Nucl. Phys. A282 (1977) 341.
37) M. Cahay, J. Cugnon, J. Vandermeulen, Nucl. Phys. A411 (1983) 524.
38) R. Malfliet, to be published.
39) D. Enskog, Kungl. Svenska Vet. Akad. Handl. 63 (1921) n° 4.
40) T. Hamada, I.D. Johnston, Nucl. Phys. 34 (1962) 382.
41) E.C. Halbert, Phys. Rev. C23 (1981) 295.